Ionics
DOI 10.1007/s11581-013-0975-1

ORIGINAL PAPER

Effect of temperature on lithium-ion intercalation kinetics of $LiMn_{1.5}Ni_{0.5}O_4$-positive-electrode material

Ting-Feng Yi · Shuang-Yuan Yang · Hong-Tao Ma · Xiao-Ya Li · Yong-Quan Ma · Hong-Bin Qiao · Rong-Sun Zhu

Received: 4 July 2013 / Revised: 23 July 2013 / Accepted: 26 July 2013

Abstract $LiMn_{1.5}Ni_{0.5}O_4$ is synthesized by a sol–gel method and the intercalation kinetics as positive electrode for lithium-ion batteries is investigated by EIS. $LiMn_{1.5}Ni_{0.5}O_4$ particles prepared via sol–gel process possess spinel phase with Fd-3m space group. The charge-transfer resistance, the exchange-current density and the solid-phase diffusion are found as a function of temperature. The apparent activation energy of the exchange current, the charge transfer, and the lithium diffusion in solid phase are also determined, respectively. This result indicates that the effect of the temperature on the cell capacity and the current dependence of the capacity results mainly from the enhancement of the lithium diffusion at elevated temperatures. It can be concluded that $LiMn_{1.5}Ni_{0.5}O_4$ cell has a bad rate cycling performance at elevated temperatures before any modification due to the high diffusion apparent activation energy. The relevant theoretical elucidations thus provide us some useful insights into the design of novel $LiMn_{1.5}Ni_{0.5}O_4$-based positive-electrode materials.

Keywords Lithium-ion battery · Positive-electrode material · $LiMn_{1.5}Ni_{0.5}O_4$ · Intercalation kinetics

T.-F. Yi · S.-Y. Yang · X.-Y. Li · Y.-Q. Ma · H.-B. Qiao (✉) · R.-S. Zhu
School of Chemistry and Chemical Engineering, Anhui University of Technology, Maanshan, Anhui 243002, People's Republic of China
e-mail: qiaohb@ahut.edu.cn

T.-F. Yi
Postdoctoral Research Station of Chemical Engineering and Technology, Harbin Institute of Technology, 150001 Harbin, China

T.-F. Yi (✉) · H.-T. Ma
Chilwee Power Co., Ltd, Changxing, Zhejiang 313100, People's Republic of China
e-mail: tfyihit@163.com

Introduction

In recent years, there has been much interest in the development of lithium-ion batteries having lithium insertion materials as positive electrodes. Spinel $LiMn_2O_4$ has been considered a promising positive-electrode material for lithium-ion batteries in electric vehicles, plug-in hybrid electric vehicles, and hybrid electric vehicles due to its low cost, low toxicity, and relatively high energy density [1–3]. However, poor rate capability and high-temperature performance limit its further application for high-performance rechargeable batteries before any materials modifications. The performance of $LiMn_2O_4$ has recently been significantly improved by the approaches including coating [4], particle size reduction [5, 6], and cation doping [7–14]. For cation doping, most works focused on the Mn-site substitution, and various cations such as Mg^{2+} [7], Ni^{2+} [8], Al^{3+} [9], Co^{3+} [10], Fe^{3+} [11], Cr^{3+} [12], Ti^{4+} [13], Nb^{5+} [14], and their combination have been attempted. The development of positive-electrode materials with high energy density is a crucial step to promote the applications of Li-ion batteries in high-power electronic equipments. Among all doped $LiMn_2O_4$, $LiMn_{1.5}Ni_{0.5}O_4$ has been considered as an important candidate for this purpose as it offers high working potential (4.7 V), high energy density (the energy density of $LiMn_{1.5}Ni_{0.5}O_4$ is 20 % higher than that of $LiCoO_2$), acceptable stability, and good cycling performance [4].

A variety of methods had been used to prepare $LiMn_{1.5}Ni_{0.5}O_4$ yet, such as solid-state reaction [15], sol–gel [16], emulsion drying [17], composite carbonate process [18], molten salt [19], combustion, and ultrasonic spray pyrolysis method [20].

The sol–gel method gives the electrode material with a fine particle size, a narrow size distribution, and uniform composition, which leads to high electrochemical performance, so it has been widely used to prepare positive-electrode materials of lithium-ion batteries [21]. The diffusion rate of Li^+ in solid-

Published online: 19 September 2013

state active material may control the rate determining step of the intercalation process, and plays a very important role in the study of electrodes materials for lithium-ion batteries. Hence, the lithium chemical diffusion coefficient (D_{Li}) is considered as one of the most important kinetic characteristics of electrode material. Several techniques including cyclic voltammetry [22, 23], electrochemical impedance spectroscopy (EIS) [24, 25], galvanostatic intermittent titration technique [26, 27], and capacity intermittent titration technique [28] have been extensively used to study the diffusion kinetics of Li^+ intercalation/deintercalation and to estimate the chemical diffusion coefficients of Li^+ in solid electrodes. EIS is considered as a very powerful technology to determine the rate of individual electrode kinetic steps because it can be also obtained under more equilibrium conditions compared with other methods. Hence, in order to increase the understanding of the performance limitations of $LiMn_{1.5}Ni_{0.5}O_4$, we believe that it is of utmost importance to further examine, in detail, the kinetic properties of these types of insertion electrodes over a broad range of temperatures. In the presented paper, $LiMn_{1.5}Ni_{0.5}O_4$ is successfully synthesized by a sol–gel method, and the electrochemical properties such as the charge-transfer resistance, exchange-current density, chemical diffusion coefficient, activation energy, and with different storage temperatures are evaluated using EIS.

Experiment

Analytically pure grade lithium acetate [$LiOOCCH_3 \cdot 2H_2O$] (AR, 99 %), Manganese acetate [$Mn(CH_3COO)_2 \cdot 4H_2O$] (AR, 99 %) and nickel acetate [$Ni(CH_3COO)_2 \cdot 4H_2O$] (AR, 99 %) were used as precursor materials. The stoichiometric ratios of these metallic salts were dissolved separately in citric acid at 1:1 molar ratios between the total metal ions and citric acid, followed by continuous stirring for about 1 h. Afterwards, all solutions were mixed and heated at 80 °C, followed by continuous stirring. The resulting solution was dried overnight at about 100 °C to get precursor. The obtained powders were fired at 450 °C for 4 h in air for complete organic removal. The powders after organic removal were calcined at 850 °C for 18 h in air.

The phase formation behavior of the calcined powder was characterized by XRD, using Cu Kα radiation. Electrochemical impedance spectroscopy (EIS) in two-electrode cells is measured by a PARSTAT 4000 electrochemical working station over a frequency range from 0.1 Hz to 10 kHz at a potentiostatic signal amplitude of 5 mV. The difference between two-electrode system and three-electrode system is that the impedance spectrum of the two-electrode system is equal to the sum of the spectra of the positive and the negative electrodes in a three-electrode system [29, 30]. The prepared electrode materials were adopted as the work electrode; the counter electrode and reference electrode were Li foil. The positive electrode was prepared by mixing above active material, carbon black, and polyvinylidene fluoride in a weight ratio of (80:10:10) and emulsified in *N*-methyl-2-pyrrolidone. The resulting paste was spread on Al foil and dried overnight at about 120 °C. The CR 2032 coin cell was prepared in an Ar atmosphere inside a glove box using Li metal foil as anode and electrolyte consisting of 1 M $LiPF_6$, dissolved in ethylene carbonate and diethyl carbonate (1:1 volume ratio). The working electrode and Li metal foil were separated using Cellgard 2400 membrane.

Results and discussion

XRD pattern of the as-prepared $LiMn_{1.5}Ni_{0.5}O_4$ samples is displayed in Fig. 1. The identified phase is $LiMn_{1.5}Ni_{0.5}O_4$ having a cubic spinel structure and space group of Fd-3m, in which the lithium ions occupy the tetrahedral (8a Wyckoff position) sites, the transition metals Ni and Mn are located at the octahedral (16d Wyckoff position) sites, and the oxygen atoms reside in the Wyckoff position of 32e sites. It can be found that an impurity peak at about 43.5° can be observed from XRD pattern, being recognized as the weak impurity phase of $Li_xNi_{1-x}O$, which is caused by oxygen loss when the sintering temperature was above 650 °C, accompanied with a small amount Mn^{3+} generated for balance the valence [24].

Electrochemical impedance spectroscopy (EIS) are measured to get insight into the origin of the electrode kinetics of $LiMn_{1.5}Ni_{0.5}O_4$ sample. Figure 2 presents Nyquist plots of $LiMn_{1.5}Ni_{0.5}O_4$ measured at different temperatures, and the equivalent circuit used to fit the EIS and the enlarged Nyquist plots are shown in the inset of Fig. 2. The semicircle in the high-frequency region is related to the resistance (R_f) of

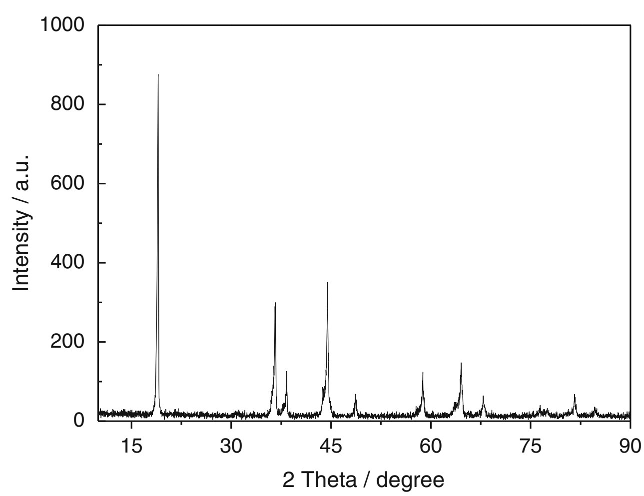

Fig. 1 X-ray diffraction patterns of pristine and modified $LiMn_{1.5}Ni_{0.5}O_4$

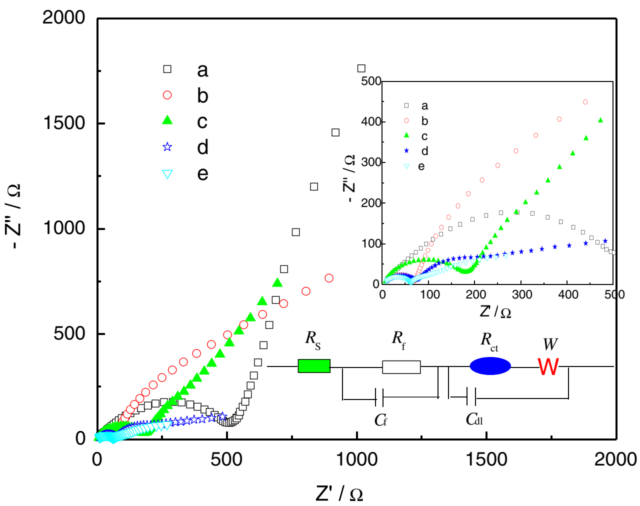

Fig. 2 Nyquist plots of $LiMn_{1.5}Ni_{0.5}O_4$ electrodes at different temperatures. *Inset* is the equivalent circuit used to fit the EIS and the enlarged Nyquist plots (*a*) 15 °C, (*b*) 25 °C, (*c*) 35 °C, (*d*) 45 °C, and (*e*) 55 °C

migration of Li^+ ions through the surface films and film capacitance (C_f) [31], and the straight line in the low-frequency region is attributed to a semi-infinite Warburg diffusion process in the bulk attributed to the diffusion of the lithium ions into the bulk of the electrode material. The middle frequency capacitive loop is caused by charge-transfer resistance (R_{ct}) and interfacial capacitance (C_{dl}). R_S is the solution ohmic resistance of the electrode system [32]. Moreover, the fitted parameter values are displayed in Table 1. It can be observed that there is no significant difference between the parameter values in the solution ohmic resistances. It can be found that the R_S values measured at all temperatures are less that 5 Ω, being in a negligible region of the deviation. The difference may be due to the fitted error. It can be concluded that the electrolyte concentration may remain invariant, and variations in the lithium content of the electrodes do not influence the electrolyte conductivity [33]. The charge-transfer resistance R_{ct} values evidently decreases with increasing of the temperature.

The exchange-current density, i_0, can be calculated by means of the charge-transfer resistance [34],

$$i_0 = \frac{RT}{nFR_{ct}} \tag{1}$$

Table 1 Kinetics parameters of $LiMn_{1.5}Ni_{0.5}O_4$ electrodes at different temperatures

Temperature, °C	15	25	35	45	55
R_s, Ω	3.247	5.347	3.619	4.239	3.736
R_{ct}, Ω	658.4	589.2	478.0	431.1	327.1
i_0, $\times 10^{-5}$ A	3.90	4.36	5.37	5.96	7.85
D_{Li}, $\times 10^{-15}$ cm^2 s^{-1}	0.105	0.499	1.668	3.261	10.76

where *R* is the gas constant, *T* the absolute temperature, *n* the number of electrons transferred in the half-reaction for the redox couple, and *F* is the Faraday constant. According to the Eq. (1), the calculated results of i_0 are shown in Table 1 as function of the temperature. Obviously, the exchange current increases with increasing of the temperature. The logarithmic i_0 is plotted against the inverse of temperature as shown in Fig. 3, and the resultant plots follow the conventional Arrhenius equation:

$$i_0 = i_A \exp\left(\frac{-Ea}{RT}\right) \tag{2}$$

where i_A is a temperature-independent coefficient. On the basis of Eq. (2), the activation energy can be derived by the following expressions:

$$E_a = -1,000Rk\ln 10 \tag{3}$$

Here, *k* is the slope of the fitting line. The activation energy of $LiMn_{1.5}Ni_{0.5}O_4$ is calculated to be 15.94 kJ mol^{-1}. This value is less than that of the reported value of spinel $LiMn_2O_4$ (65 kJ mol^{-1}) in the range $-3<T<28$ °C [35].

The relations between charge-transfer resistance and temperature can be described by [36]

$$\ln R_{ct} = 1 + \ln\frac{R}{n^2F^2C_TA_f[(M^+)(1-x)]^{(1-\alpha)}x^\alpha} + \frac{(\Delta G-R)}{R}T^{-1} \tag{4}$$

where the meanings of M^+ is the concentration of lithium ion on the surface of electrode, *R* is the gas constant, *x* is the intercalation level, C_T is the most intercalation concentration

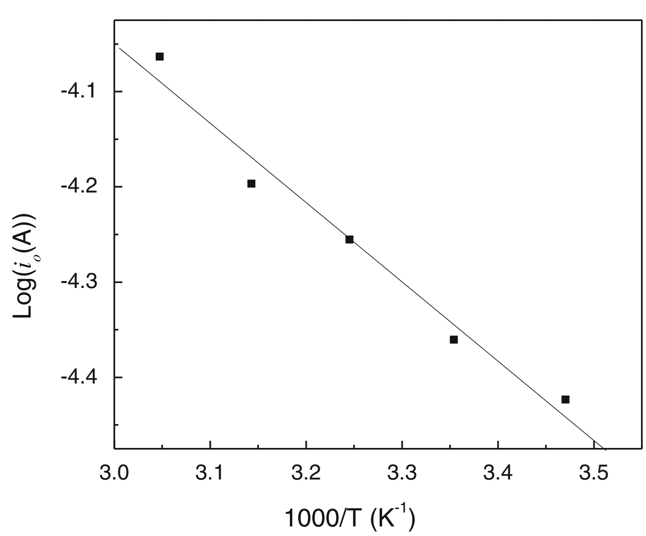

Fig. 3 Plots of log(i_o) versus 1,000/*T* for the electrodes of $LiMn_{1.5}Ni_{0.5}O_4$ materials

of lithium ions, n is the number of electrons per molecule during oxidization, a is the symmetry factor of electrochemical reaction, F is the Faraday's constant, A_f is the pre-exponential factor, and ΔG is the intercalation–deintercalation reaction active energy. The intercalation level (x) can be regarded as a constant. Hence, it can be found that there is a linear relationship between $\ln R_{ct}$ and 1,000/T as shown in Fig. 4. On the basis of Eq. (4), the intercalation–deintercalation reaction active energy can be derived by the following expressions:

$$\Delta G = R(1,000k + 1) \tag{5}$$

Here, k is the slope of the fitting line. The intercalation–deintercalation reaction activation energy of $LiMn_{1.5}Ni_{0.5}O_4$ is calculated to be 13.4 kJ mol^{-1}. This value is less than that of the reported value of spinel $LiMn_2O_4$ (53.07 kJ mol^{-1}) in the range $-10<T<30$ °C [37]. It can be concluded that $LiMn_{1.5}Ni_{0.5}O_4$ has a higher electrochemical activity than that of pristine $LiMn_2O_4$. As we know, alien cations doping at Mn-site of $LiMn_2O_4$ is a convenient and effective way to improve the electrochemical performance [38]. Hence, the reason of the doping may be due to the decreased activation energy, and then reduce the reaction energy barrier, which is the reason for the significant improvement of conductivity of $LiM_xMn_{2\text{-}x}O_4$ compound.

The chemical diffusion coefficient of the insertion electrode materials is an important kinetic parameter to determine lithium-ion charge/discharge rate. The Warburg impedance in the low frequency is mainly corresponding to the diffusion of lithium ion in the bulk of the electrode, which has been used to determine the Li-ion diffusion coefficient in the compound. Hence, the lithium-ion diffusion coefficient could be calculated from the low-frequency plots according to the following equation [39]:

$$D_{Li} = \frac{(RT)^2}{2\left(An^2F^2C_{Li}\sigma\right)^2} \tag{6}$$

where the meanings of n is the number of electrons per molecule during oxidization, A is the surface area of the electrode, R is the gas constant, T is the absolute temperature, F is the Faraday constant, C is the concentration of lithium ion, and σ is the Warburg factor which has relationship with Z_{re} [40]:

$$Z_{re} = R_{ct} + R_s + \sigma\omega^{-\frac{1}{2}} \tag{7}$$

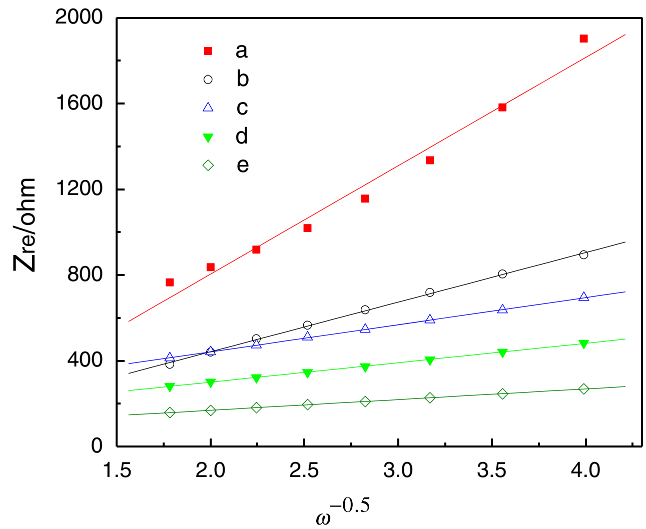

Fig. 5 Graph of Z_{re} plotted against $\omega^{-1/2}$ for $LiMn_{1.5}Ni_{0.5}O_4$ electrodes at different temperatures (*a*) 15 °C, (*b*) 25 °C, (*c*) 35 °C, (*d*) 45 °C, and (*e*) 55 °C

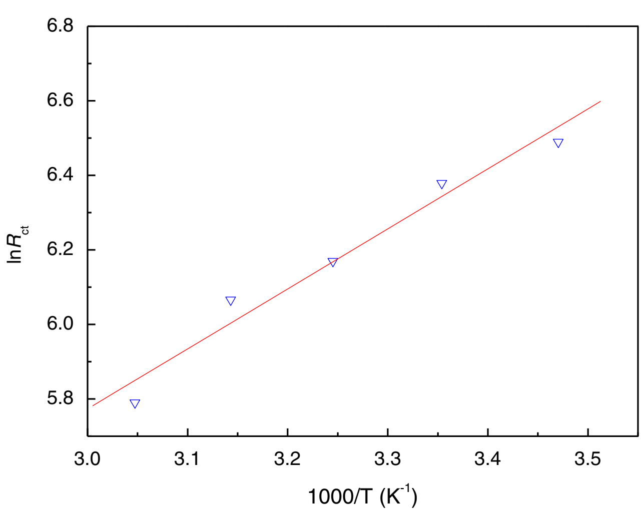

Fig. 4 Plots of $\ln R_{ct}$ versus 1,000/T for the electrodes of $LiMn_{1.5}Ni_{0.5}O_4$ materials

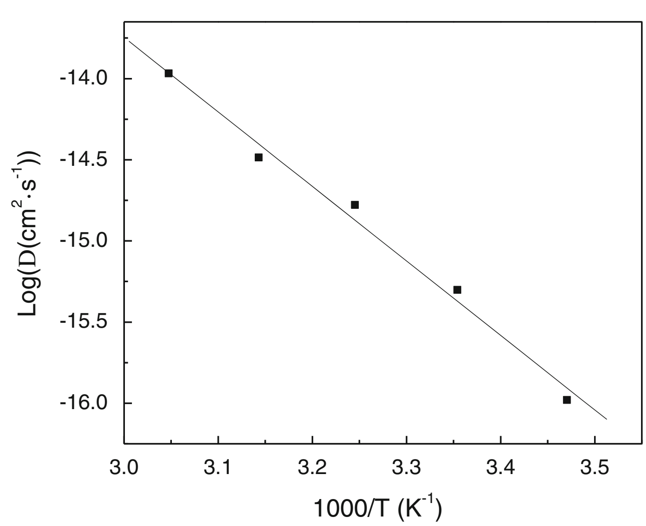

Fig. 6 Plots of log(D) versus 1,000/T for the electrodes of $LiMn_{1.5}Ni_{0.5}O_4$ materials

Figure 5 shows the relationship between Z_{re} and square root of frequency ($\omega^{-1/2}$) in the low-frequency region. The diffusion coefficient of lithium ion can be calculated based on Eqs. (6) and (7), and the calculated result is given in Table 1. It can be found that the lithium diffusion coefficient increases as temperature increases. To see more clearly the temperature effect on D_{Li}, the logarithmic D_{Li} was plotted against the inverse of temperature as given in Fig. 6, and good linearity is also observed. The resultant plots follow the conventional Arrhenius equation [41]:

$$D_{Li} = D_A \exp\left(-\frac{E_a}{RT}\right) \tag{8}$$

where D_A is the pre-exponential factor (a temperature-independent coefficient). The diffusion apparent activation energy (E_{aD}) can be calculated from the plot of log D_{Li} vs 1,000/T using equation

$$Ea_D = 1,000Rkln10 \tag{9}$$

where k is the slope of the fitting line in Fig. 6. The diffusion apparent activation energy can be calculated about 87.86 kJ mol^{-1}. This value is greater than that for the activation energy obtained by charge transfer. This result indicates that the influence of the temperature on the lithium diffusion process is larger than that of the charge transfer for the lithium extraction reaction of the $LiMn_{1.5}Ni_{0.5}O_4$ electrode. It can be concluded that the effect of the cell temperature on the cell capacity and the current dependence of the capacity results mainly from the enhancement of the lithium diffusion at elevated temperatures [42]. As we know, high rate cycling behavior is one of the most important electrochemical characteristics of lithium-ion batteries for the power storage application. It has been reported that the diffusion overpotential is lower than the charge-transfer overpotential at low discharge current densities but becomes more dominant at higher current densities, indicating that the high-rate discharge ability is mainly controlled by the diffusion behavior rather than by the charge-transfer reaction [43]. Hence, it can be concluded that $LiMn_{1.5}Ni_{0.5}O_4$ cell has a bad rate cycling performance at elevated temperatures before any modification due to the high diffusion apparent activation energy, which is consistent with the reported experimental results [44, 45]. The relevant theoretical elucidations thus provide us some useful insights into the design of novel $LiMn_{1.5}Ni_{0.5}O_4$-based positive-electrode materials.

Conclusions

$LiMn_{1.5}Ni_{0.5}O_4$-positive-electrode material was successfully synthesized by a sol–gel method. XRD patterns of $LiMn_{1.5}Ni_{0.5}O_4$ could be assigned to a spinel structure with Fd-3m space group. The electrolyte concentration remains invariant, and variations in the lithium content of the electrodes do not influence the electrolyte conductivity. $LiMn_{1.5}Ni_{0.5}O_4$ has a higher electrochemical activity than that of pristine $LiMn_2O_4$ due to the small apparent activation energy of the exchange current and the charge transfer compared with the reported value of spinel $LiMn_2O_4$. The high-rate discharge ability is mainly controlled by the diffusion behavior rather than by the charge-transfer reaction, indicating that $LiMn_{1.5}Ni_{0.5}O_4$ cell has a bad rate cycling performance at elevated temperatures before any modification due to the high diffusion apparent activation energy. The relevant theoretical elucidations thus provide us some useful insights into the design of novel $LiMn_{1.5}Ni_{0.5}O_4$-based positive-electrode materials.

Acknowledgments This work was financially supported by the National Natural Science Foundation of China (no. 51274002) the China Postdoctoral Science Foundation funded project (no. 2012M520749), the Zhejiang Postdoctoral Preferential Foundation (no. Bsh1201013), and the Program for Innovative Research Team in Anhui University of Technology (no. TD201202).

References

1. Yao J, Lv L, Shen C, Zhang P, Aguey-Zinsou K-F, Wang L (2013) Nano-sized spinel $LiMn_2O_4$ powder fabricated *via* modified dynamic hydrothermal synthesis. Ceram Int 39:3359–3364
2. Xiao L, Guo Y, Qu D, Deng B, Liu H, Tang D (2013) Influence of particle sizes and morphologies on the electrochemical performances of spinel $LiMn_2O_4$ cathode materials. J Power Sources 225:286–292
3. Wang Y, Cao G (2008) Developments in nanostructured cathode materials for high-performance lithium-ion batteries. Adv Mater 20:2251–2269
4. Yi T-F, Zhu Y-R, Zhu X-D, Shu J, Yue C-B, Zhou A-N (2009) A review of recent developments in the surface modification of $LiMn_2O_4$ as cathode material of power lithium-ion battery. Ionics 15:779–784
5. Tang SB, Lai MO, Lu L (2007) Electrochemical studies of low-temperature processed nano-crystalline $LiMn_2O_4$ thin film cathode at 55 °C. J Power Sources 164:372–378
6. Doi T, Yahiro T, Okada S, Yamaki J-i (2008) Electrochemical insertion and extraction of lithium-ion at nano-sized $LiMn_2O_4$ particles prepared by a spray pyrolysis method. Electrochim Acta 53:8064–8069
7. Song G-M, Li W-J, Zhou Y (2004) Synthesis of Mg-doped $LiMn_2O_4$ powders for lithium-ion batteries by rotary heating. Mater Chem Phys 87:162–167
8. Wang FX, Xiao SY, Shi Y, Liu LL, Zhu YS, Wu YP, Wang JZ, Holze R (2013) Spinel $LiNi_xMn_{2-x}O_4$ as cathode material for aqueous rechargeable lithium batteries. Electrochim Acta 93:301–306
9. Lee J-F, Tsai Y-W, Santhanam R, Hwang BJ, Yang M-H, Li D-G (2003) Local structure transformation of nano-sized Al-doped $LiMn_2O_4$ sintered at different temperatures. J Power Sources 119–121:721–726

10. Shen CH, Liu RS, Gundakaram R, Chen JM, Huang SM, Chen JS, Wang CM (2001) Effect of Co doping in $LiMn_2O_4$. J Power Sources 102:21–28
11. Choi H-J, Lee K-M, Lee J-G (2001) $LiMn_{1.95}M_{0.05}O_4$ (M: Al, Co, Fe, Ni, Y) cathode materials prepared by combustion synthesis. J Power Sources 103:154–159
12. Churikov AV, Romanova VO (2012) An electrochemical study on the substituted spinel $LiMn_{1.95}Cr_{0.05}O_4$. Ionics 18:837–844
13. Xiong L, Xu Y, Tao T, Goodenough JB (2012) Synthesis and electrochemical characterization of multi-cations doped spinel $LiMn_2O_4$ used for lithium ion batteries. J Power Sources 199:214–219
14. Yi T-F, Yin L-C, Ma Y-Q, Shen H-Y, Zhu Y-R, Zhu R-S (2013) Lithium-ion insertion kinetics of Nb-doped $LiMn_2O_4$ positive-electrode material. Ceram Int 39:4673–4678
15. Chen ZY, Ji S, Linkov V, Zhang JL, Zhu W (2009) Performance of $LiNi_{0.5}Mn_{1.5}O_4$ prepared by solid-state reaction. J Power Sources 189:507–510
16. Shi JY, Yi C-W, Kim K (2010) Improved electrochemical performance of $AlPO_4$-coated $LiMn_{1.5}Ni_{0.5}O_4$ electrode for lithium-ion batteries. J Power Sources 195:6860–6866
17. Myung ST, Komaba S, Kumagai N, Yashiro H, Chung HT, Cho TH (2002) Nano-crystalline $LiNi_{0.5}Mn_{1.5}O_4$ synthesized by emulsion drying method. Electrochim Acta 47:2543–2549
18. Lee YS, Sun YK, Ota S, Miyashita T, Yoshio M (2002) Preparation and characterization of nano-crystalline $LiNi_{0.5}Mn_{1.5}O_4$ for 5 V cathode material by composite carbonate process. Electrochem Commun 4:989–994
19. Kim JH, Myung ST, Sun YK (2004) Molten salt synthesis of $LiNi_{0.5}Mn_{1.5}O_4$ spinel for 5 V class cathode material of Li-ion secondary battery. Electrochim Acta 49:219–227
20. Julien CM, Mauger A (2013) Review of 5-V electrodes for Li-ion batteries: status and trends. Ionics 19:951–988
21. Fu LJ, Liu H, Li C, Wu YP, Rahm E, Holze R, Wu HQ (2005) Electrode materials for lithium secondary batteries prepared by sol–gel methods. Prog Mater Sci 50:881–928
22. Zhao G, Lin Y, Zhou T, Lin Y, Huang Y, Huang Z (2012) Enhanced rate and high-temperature performance of $La_{0.7}Sr_{0.3}MnO_3$-coated $LiNi_{0.5}Mn_{1.5}O_4$ cathode materials for lithium ion battery. J Power Sources 215:63–68
23. Rui XH, Yesibolati N, Li SR, Yuan CC, Chen CH (2011) Determination of the chemical diffusion coefficient of Li^+ in intercalation-type $Li_3V_2(PO_4)_3$ anode material. Solid State Ionics 187:58–63
24. Nie X, Zhong B, Chena M, Yina K, Li L, Liu H, Guo X (2013) Synthesis of $LiCr_{0.2}Ni_{0.4}Mn_{1.4}O_4$ with superior electrochemical performance via a two-step thermo polymerization technique. Electrochim Acta 97:184–191
25. Hjelm A-K, Lindbergh G (2002) Experimental and theoretical analysis of $LiMn_2O_4$ cathodes for use in rechargeable lithium batteries by electrochemical impedance spectroscopy (EIS). Electrochim Acta 47:1747–1759
26. Deiss E (2005) Spurious chemical diffusion coefficients of Li^+ in electrode materials evaluated with GITT. Electrochim Acta 50:2927–2932
27. Xie J, Kohno K, Matsumura T, Imanishi N, Hirano A, Takeda Y, Yamamoto O (2008) Li-ion diffusion kinetics in $LiMn_2O_4$ thin films prepared by pulsed laser deposition. Electrochim Acta 54:376–381
28. Tang X-C, Song X-W, Shen P-Z, Jia D-Z (2005) Capacity intermittent titration technique (CITT): a novel technique for determination of Li^+ solid diffusion coefficient of $LiMn_2O_4$. Electrochim Acta 50:5581–5587
29. Zhang S, Shi P (2004) Electrochemical impedance study of lithium intercalation into MCMB electrode in a gel electrolyte. Electrochim Acta 49:1475–1482
30. Song JY, Lee HH, Wang YY, Wan CC (2002) Two- and three-electrode impedance spectroscopy of lithium-ion batteries. J Power Sources 111:255–267
31. Levi MD, Aurbach D (1997) Simultaneous measurements and modeling of the electrochemical impedance and the cyclic voltammetric characteristics of graphite electrodes doped with lithium. J Phys Chem B 101:4630–4640
32. Wu HM, Belharouak I, Abouimrane A, Sun Y-K, Amine K (2010) Surface modification of $LiNi_{0.5}Mn_{1.5}O_4$ by ZrP_2O_7 and ZrO_2 for lithium-ion batteries. J Power Sources 195:2909–2913
33. Fey GT-K, Lu C-Z, Kumar TP (2003) Preparation and electrochemical properties of high-voltage cathode materials, $LiM_yNi_{0.5-y}Mn_{1.5}O_4$ (M = Fe, Cu, Al, Mg; y=0.0–0.4). J Power Sources 115:332–345
34. Zhou X, Zou Y, Yang J (2013) Carbon supported tin-based nanocomposites as anodes for Li-ion batteries. J Solid State Chem 198:231–237
35. Hjelm A-K, Eriksson T, Lindbergh G (2002) Electrochemical investigation of $LiMn_2O_4$ cathodes in gel electrolyte at various temperatures. Electrochim Acta 48:171–179
36. Zhuang QC, Xu JM, Fan XY, Wei GZ, Dong QF, Sun SG (2008) Effects of temperature on the process of lithium intercalation-deintercalation in $LiCoO_2$. Acta Chim Sin 66:722–728
37. Tao W, Zhuang QC, Wu C, Cui YL, Fang L, Sun SG (2010) Effects of temperature on the intercalation-deintercalation process of lithium ion in the spinel $LiMn_2O_4$. Acta Chim Sin 68:1481–1486
38. Fergus JW (2010) Recent developments in cathode materials for lithium ion batteries. J Power Sources 195:939–954
39. Liu H, Cao Q, Fu LJ, Li C, Wu YP, Wu HQ (2006) Doping effects of zinc on $LiFePO_4$ cathode material for lithium ion batteries. Electrochem Commun 8:1553–1557
40. Sarkar S, Banda H, Mitra S (2013) High capacity lithium-ion battery cathode using LiV_3O_8 nanorods. Electrochim Acta 99:242–252
41. Zhu Y-R, Yin L-C, Yi T-F, Liu H, Xie Y, Zhu R-S (2013) Electrochemical performance and lithium-ion intercalation kinetics of submicron-sized $Li_4Ti_5O_{12}$ anode material. J Alloys Compd 547:107–112
42. Takahashi M, Tobishima S-i, Takei K, Sakurai Y (2002) Reaction behavior of $LiFePO_4$ as a cathode material for rechargeable lithium batteries. Solid State Ionics 148:283–289
43. Wu M-S, Chiang P-C J, Lin J-C (2005) Electrochemical investigations on advanced lithium-ion batteries by three-electrode measurements. J Electrochem Soc 152:A47–A52
44. Sun Y-K, Hong K-J, Prakash J, Amine K (2002) Electrochemical performance of nano-sized ZnO-coated $LiNi_{0.5}Mn_{1.5}O_4$ spinel as 5 V materials at elevated temperatures. Electrochem Commun 4:344–348
45. Yoon T, Park S, Mun J, Ryu JH, Choi W, Kang Y-S, Park J-H, Oh SM (2012) Failure mechanisms of $LiNi_{0.5}Mn_{1.5}O_4$ electrode at elevated temperature. J Power Sources 215:312–316